

A STATE-SPACE MODELING OF NON-IDEAL DC-DC CONVERTERS

C. T. Rim, G. B. Joung and G. H. Cho

Dept. of Electrical Engineering, Korea Advanced Institute of Science and Technology

P.O.Box 150 Chongryang, Seoul 131, Korea (Tel. 966-1931 ext. 3723)

ABSTRACT

A modeling based on the practical switches with finite turn-on, turn-off, delay, storage and reverse recovery times is proposed. The switching effects on the state equation, system stability, dc gain and efficiency are shown for the boost, buck and buck-boost converters. The effect of switching time variation by current on system stability is given as an extension of the storage time modulation effect. And the effect of average duty cycle variation on system stability is newly introduced. DC gains of the boost and buck-boost converters are shown to be much deteriorated by switching loss. It is also shown that no additional resistance is generated by switching in contradiction to previous work. Besides, it is found that buck converter is superior to others from the viewpoints of the system stability and dc gain, and the efficiencies of all the converters are maximized when the dc gain is close to unity. Previous related papers are improved and unified using a new state-space modeling. Analysis results are very simple in spite of the complex switching waveforms. This new modeling is believed to be very useful for the high frequency or high power applications where switching effects become dominant.

I. INTRODUCTION

The modeling of networks which contain switches has drawn much attention because of the unusual properties of switches in comparison with other circuit elements. This is the reason why there are so many modelings in the power electronics which are not found in other fields.

The difficulties in the modeling of switched networks are mainly due to the non-linear and time-varying nature of switches. Furthermore the control mechanism of switching systems is far different from ordinary systems. The difference is shown in Fig. 1. By switching, the topologies of networks are changed and the system matrices A, B, C and D are, accordingly, changed. So to control the output of switching systems, the system matrices should be varied by switches instead of the source as done in ordinary systems. This is why switching systems are non-linear and time-varying.

Most modelings in power electronics are mainly intended to convert this non-linear time-varying problem to an easier form [1-5]. However they are inadequate for some delicate problems since they are based on ideal switches. So a few papers based on non-ideal switches are proposed [6-9]. Focusing on the switching effects for the related previous works, the storage time modulation effect on small signal dynamics is found in [6]. And switching time effect on efficiency assuming ideal filters is investigated in detail in [7]. A substitution of switching effect to an equivalent resistance is done in [8]. Switching effect on dc gain degeneration is discussed in [9].

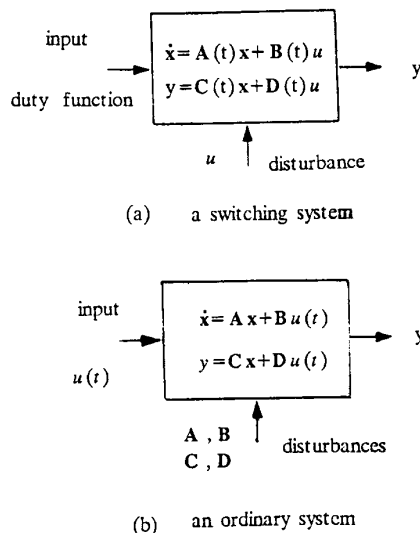


Fig. 1 Comparison of systems.

However they explain only parts of switching effects with somewhat rough or complex expressions.

This paper is intended to unify and extend the previous works so that this may be a good summary for switching effects on power systems. A new state space modeling is proposed to obtain both exact and simple results, which are believed to be the most important features of system modelings. Conventional state space average modeling is based on two or three sets of state equations which are valid for each mode. So this is inadequate for the representation of the interval between successive modes which appears in the practical switching case. Here a time-varying state equation valid not only for each mode but also for the interval between modes is set up using switching functions with little effort. Then more extended and compact state-space averaging and perturbations are taken for the boost converter example. The state-space analyses for the system stability, dc gain and efficiency for three converters are done and the results are summarized in a table.

II. MODELING PROCEDURE
(BOOST CONVERTER CASE)

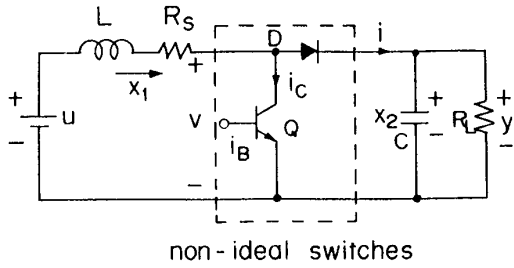


Fig. 2 Boost converter.

The modeling procedure is shown for the boost converter case. It is assumed that all the passive elements are LTI and that the switches have only switching loss. The conduction loss and parasitic resistance loss will be counted in the Part II of this paper in later. The converter is assumed to operate in the continuous conduction mode. Fig. 2 shows the circuit to be modeled and Fig. 3 shows the switching waveforms, respectively.

A. Exact State-Space Model

To derive a state equation, states x_1 and x_2 are allocated to the current of inductor L and the voltage of capacitor C , respectively. Then the derivatives of the states as functions of states, source and circuit parameters are found to be

$$L \dot{x}_1 = u - R_s x_1 - v, \quad C \dot{x}_2 = i - \frac{x_2}{R_L} \quad (1)$$

Note that this state equation is valid also for the non-ideal switch case where the switching waveform can be arbitrary. What remains is v and i to be expressed as functions of already known variables. From the switching waveforms it can be seen that v and i are the switched portions of x_2 and x_1 , respectively.

$$v = s_1(t) x_2, \quad i = s_2(t) x_1 \quad (2)$$

where $s_1(t), s_2(t)$ are defined as the switching functions determined by

$$s_1(t) = \frac{v}{x_2}, \quad s_2(t) = \frac{i}{x_1} \quad (3)$$

The switching functions are shown in Fig. 4. Provided that the switching times are known then the switching functions are fully determined.

By applying (2) to (1) and rearranging it, the state equation and the output equation of the boost converter are obtained.

$$\begin{bmatrix} \dot{x}_1 \\ \dot{x}_2 \end{bmatrix} = \begin{bmatrix} \frac{R_s}{L} & -\frac{s_1(t)}{L} \\ \frac{s_2(t)}{C} & -\frac{1}{C R_L} \end{bmatrix} \begin{bmatrix} x_1 \\ x_2 \end{bmatrix} + \begin{bmatrix} \frac{1}{L} \\ 0 \end{bmatrix} u \quad y = [0 \ 1] \begin{bmatrix} x_1 \\ x_2 \end{bmatrix} \quad (4)$$

(4) is of the form

$$\dot{x} = A(t)x + B u, \quad y = C x \quad (5)$$

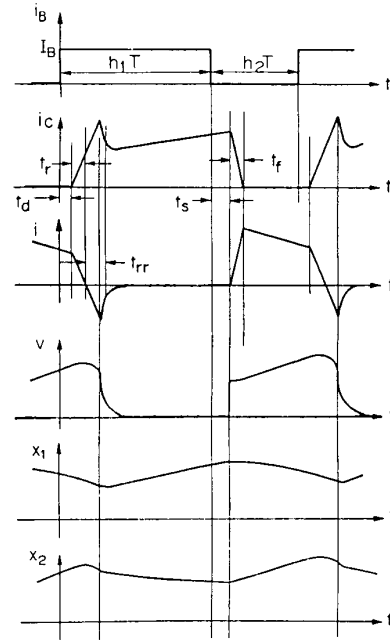


Fig. 3 Switching waveforms of boost converter.

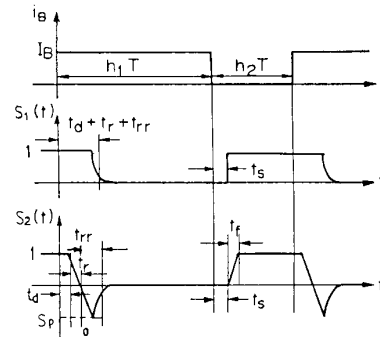


Fig. 4 Switching functions $s_1(t)$ and $s_2(t)$

Note that the exact model of the converter is of time-varying form, which is the general property of switching systems. This new model is exact enough to be used for simulations.

B. State - Space Averaging and Perturbation

To eliminate the time-varying terms in the matrices $A(t), B(t)$ and $C(t)$, a generalized state-space averaging is taken for them as

$$\dot{x} = \bar{A} x + \bar{B} u, \quad y = \bar{C} x \quad (6)$$

where

$$\bar{\mathbf{A}} = \frac{1}{T} \int_0^T \mathbf{A}(t) dt, \quad \bar{\mathbf{B}} = \frac{1}{T} \int_0^T \mathbf{B}(t) dt, \quad \bar{\mathbf{C}} = \frac{1}{T} \int_0^T \mathbf{C}(t) dt \quad (7)$$

In the boost converter case the matrices are evaluated as

$$\bar{\mathbf{A}} = \begin{bmatrix} -\frac{R_s}{L} & -\frac{s_1}{L} \\ \frac{s_2}{C} & -\frac{1}{CR_L} \end{bmatrix}, \quad \bar{\mathbf{B}} = \begin{bmatrix} 1 \\ 0 \end{bmatrix}, \quad \bar{\mathbf{C}} = [0 \ 1] \quad (8)$$

The s_1 and s_2 are the averages of $s_1(t)$ and $s_2(t)$, respectively. They are evaluated from Fig. 4 as

$$s_1 = \frac{1}{T} \int_0^T s_1(t) dt = 1 - h + t_1 f \quad \text{for } H_{\min} < h < H_{\max} \quad (9a)$$

$$s_2 = \frac{1}{T} \int_0^T s_2(t) dt = 1 - h + t_2 f \quad \text{for } H_{\min} < h < H_{\max} \quad (9b)$$

where

Q; t_d : delay time, t_r : rise time, t_f : fall time, t_s : storage time, D; t_{rr} : reverse recovery time, s_p : reverse peak, h : duty factor,

$$h = h_1 = 1 - h_2, \quad t_1 = t_d + t_r + t_{rr} - t_s, \quad t_2 = t_d + \frac{t_r}{2} - \tau - t_s - \frac{t_f}{2},$$

$$f = \frac{1}{T}, \quad H_{\min} = (t_d + t_r + t_{rr})/T, \quad H_{\max} = 1 - (t_s + t_f - t_d)/T \quad (10)$$

H_{\min} , H_{\max} are determined by the turn-on, off overlap conditions of the switches. And τ is introduced assuming that the diode reverse recovery charge Q_{rr} is proportional to its forward current as

$$\begin{aligned} Q_{rr} &= - \int_0^{t_{rr}} i_D(t) dt = - \int_0^{t_{rr}} x_1(t) s_1(t) dt \approx -x_1(t) \frac{s_p t_{rr}}{2} \\ &= \tau x_1(t) \quad \text{or} \quad \tau = - \frac{s_p t_{rr}}{2} \end{aligned} \quad (11)$$

The inductor current $x_1(t)$ has been assumed to be constant and the τ is found to be the life time of the minority carrier.

Assuming that the switching times are non-linear function of the inductor current and the \mathbf{C} matrix is constant, then (6) becomes

$$\dot{\mathbf{x}} = \mathbf{A}(h, \mathbf{x}) \mathbf{x} + \mathbf{B}(h, \mathbf{x}) u, \quad \mathbf{y} = \mathbf{C}_0 \mathbf{x} \quad (12)$$

To eliminate the non-linearity in (12), matrices are expanded in power series neglecting higher order terms as

$$\begin{aligned} \mathbf{A}(h, \mathbf{x}) &\approx \mathbf{A}(H_0, X_1) + \frac{\partial \mathbf{A}(h, \mathbf{x})}{\partial h} \Big|_{h=H_0} (h - H_0) + \\ \frac{\partial \mathbf{A}(h, \mathbf{x})}{\partial x_1} \Big|_{x_1=X_1} (x_1 - X_1) &= \mathbf{A}_0 + \mathbf{A}_1 \cdot (h - H_0) + \mathbf{A}_2 \cdot (x_1 - X_1) \end{aligned} \quad (13a)$$

and

$$\mathbf{B}(h, \mathbf{x}) = \mathbf{B}_0 + \mathbf{B}_1 \cdot (h - H_0) + \mathbf{B}_2 \cdot (x_1 - X_1) \quad (13b)$$

Applying (13) to (12) and taking the following perturbations

$$h = H_0 + \hat{h}, \quad \mathbf{x} = \mathbf{X}_0 + \hat{\mathbf{x}}, \quad \mathbf{y} = Y_0 + \hat{\mathbf{y}} \quad (14)$$

the resultant equations become

$$\begin{aligned} (\dot{\mathbf{X}}_0 + \dot{\hat{\mathbf{x}}}) &= (\mathbf{A}_0 + \mathbf{A}_1 \hat{h} + \mathbf{A}_2 \hat{x}_1) (\mathbf{X}_0 + \hat{\mathbf{x}}) + (\mathbf{B}_0 + \mathbf{B}_1 \hat{h} + \mathbf{B}_2 \hat{x}_1) U_0 \\ (Y_0 + \hat{\mathbf{y}}) &= \mathbf{C}_0 (\mathbf{X}_0 + \hat{\mathbf{x}}) \end{aligned} \quad (15)$$

Ignoring bilinear terms, (15) is separated into the dc and ac parts as

$$\dot{\mathbf{X}}_0 = \mathbf{A}_0 \mathbf{X}_0 + \mathbf{B}_0 U_0, \quad Y_0 = \mathbf{C}_0 \mathbf{X}_0 \quad (16)$$

and

$$\begin{aligned} \dot{\hat{\mathbf{x}}} &= (\mathbf{A}_0 + \mathbf{A}_2 \mathbf{X}_0 \mathbf{W} + \mathbf{B}_2 U_0 \mathbf{W}) \hat{\mathbf{x}} + (\mathbf{A}_1 \mathbf{X}_0 + \mathbf{B}_1 U_0) \hat{h} \\ \hat{\mathbf{y}} &= \mathbf{C}_0 \hat{\mathbf{x}} \end{aligned} \quad (17)$$

where \mathbf{W} is defined as

$$\mathbf{W} = [1 \ 0] \quad (18)$$

From (16), operating point Y_0 is determined by setting $\dot{\mathbf{X}}_0$ to zero as follows:

$$\mathbf{A}_0 \mathbf{X}_0 + \mathbf{B}_0 U_0 = 0, \quad Y_0 = -\mathbf{C}_0 \mathbf{A}_0^{-1} \mathbf{B}_0 U_0 \quad (19)$$

From (17), the transfer function $G(s)$ is determined as

$$\begin{aligned} G(s) = \frac{\hat{Y}(s)}{\hat{H}(s)} &= \mathbf{C}_0 (s\mathbf{I} - \mathbf{A}_0 - \mathbf{A}_2 \mathbf{X}_0 \mathbf{W} - \mathbf{B}_2 U_0 \mathbf{W})^{-1} \\ &\quad \cdot (\mathbf{A}_1 \mathbf{X}_0 + \mathbf{B}_1 U_0) \end{aligned} \quad (20)$$

System stability can be evaluated by examining the characteristic equation

$$|s\mathbf{I} - \mathbf{A}_0 - \mathbf{A}_2 \mathbf{X}_0 \mathbf{W} - \mathbf{B}_2 U_0 \mathbf{W}| = 0 \quad (21)$$

In the boost converter case, the matrices, $\mathbf{A}_0, \mathbf{A}_1, \dots, \mathbf{C}_0$ are found to be

$$\mathbf{A}_0 = \begin{bmatrix} -\frac{R_s}{L} & -\frac{1-H_0+t_1f}{L} \\ \frac{1-H_0+t_2f}{C} & -\frac{1}{CR_L} \end{bmatrix}, \quad \mathbf{A}_1 = \begin{bmatrix} 0 & \frac{1}{L} \\ -\frac{1}{C} & 0 \end{bmatrix},$$

$$\mathbf{A}_2 = \begin{bmatrix} 0 & -\frac{f}{L} \frac{dt_1}{dx_1} \\ \frac{f}{C} \frac{dt_2}{dx_1} & 0 \end{bmatrix}$$

$$\mathbf{B}_0 = \begin{bmatrix} 1 \\ L \\ 0 \end{bmatrix}, \quad \mathbf{B}_1 = \mathbf{B}_2 = 0, \quad \mathbf{C}_0 = [0 \ 1] \quad (22)$$

C. Pole Frequency Deviation Effect

By applying (22) to (21) poles are found to be

$$\begin{aligned} s^2 + \left(\frac{R_s^*}{L} + \frac{1}{CR_L} \right) s + \frac{(1-H_0+t_1f)(1-H_0+t_2^*f) + R_s^*/R_L}{LC} \\ = s^2 + 2\zeta \omega_n s + \omega_n^2 = 0 \end{aligned} \quad (23)$$

where

$$R_s^* = R_s + f \frac{dt_1}{dx_1} X_2, \quad t_2^* = t_2 + \frac{dt_2}{dx_1} X_1 \quad (24)$$

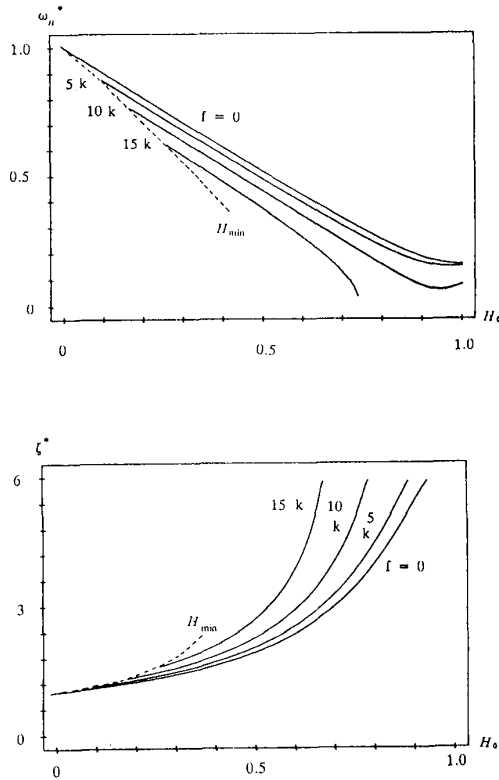


Fig. 5 Pole frequency deviation of boost converter.

It is observed that R_s and t_2 are replaced by R_s^* and t_2^* by switching time modulation. This means that the poles can be calculated as if there is no switching time modulation by substituting R_s^* and t_2^* . Note that the switching time modulation effect which is undesirable in practice becomes dominant as X_1, X_2 are increased. So it is recommended that the operating point be low to avoid the undesirable effect. It had been discussed in [6] that R_s is effectively varied by storage time modulation. That result is in part true, however, it needs to be extended as described here to give more exact solution. Still there remains another switching effect to be explained, the duty cycle variation effect. Duty cycle is moved from H_0 to $H_0 - t_1 f$ or $H_0 - t_2^* f$ as shown in (23). It is apparent that this effect will be dominant at high switching frequency.

The normalized natural frequency and normalized damping factor which are the ratios of the practical ones and the ideal ones with zero duty factor are

$$\omega_n^* = \frac{\omega_n}{\omega_n|_{t_1, t_2, H_0=0}} = \sqrt{\frac{R_s^*/R_L + (1-H_0+t_1 f)(1-H_0+t_2^* f)}{R_s^*/R_L + 1}} \quad (25a)$$

$$\zeta^* = \frac{\zeta}{\zeta|_{t_1, t_2, H_0=0}} = \sqrt{\frac{R_s^*/R_L + 1}{R_s^*/R_L + (1-H_0+t_1 f)(1-H_0+t_2^* f)}} \quad (25b)$$

ω_n^* and ζ^* are plotted in Fig. 5 for a typical power switching transistor whose current level is hundred amperes. In fact the switching times are varied by current and temperature, however, they are fixed for illustration purpose. Typical values of them and resistors selected, which are to be used throughout this paper, are as follows:

$$\begin{aligned} t_d &= 8.0 \mu s, \quad t_r = 0.6 \mu s, \quad t_{rr} = 8.5 \mu s, \quad t_s = 5.0 \mu s, \\ t_f &= 1.0 \mu s, \quad \tau = 11.0 \mu s, \quad t_1 = t_d + t_r + t_{rr} - t_s = 12.1 \mu s, \\ t_2 &= t_d + \frac{t_r}{2} - \tau - t_s - \frac{t_f}{2} = -8.2 \mu s, \quad \frac{dt_1}{dx_1} X_2 = 20 \mu s \text{ ohms}, \\ \frac{dt_2}{dx_1} X_1 &= -15 \mu s, \quad R_s = 0.50 \text{ ohms}, \quad R_L = 20 \text{ ohms}. \end{aligned} \quad (26)$$

It can be seen that system poles are non-linear to the duty factor and are considerably deviated from the ideal switching case as the switching frequency is increased. And the open loop system stability for a typical switching case is improved by switching.

The switching effect on system stability can be summarized as two effects; one is the switching time modulation effect, which results in the variation of R_s, t_2 and the other is the average duty factor modification effect, which results in the variation of average duty factor.

D. DC Gain Deviation Effect

To check the switching effect on dc gain, (19) is evaluated using (22). The dc gain G_v is then

$$G_v = \frac{Y_0}{U_0} = -C_0 A_0^{-1} B_0 = \frac{(1-H_0+t_2 f)}{\frac{R_s}{R_L} + (1-H_0+t_1 f)(1-H_0+t_2 f)} \quad (27)$$

The dc gain is shown in Fig. 6 as a function of duty factor for several switching frequencies. The switching times and resistances used here are the same as (26). Note that the practical boost converter has the maximum dc gain point which occurs at the point, H_0^* given by

$$\frac{\partial G_v}{\partial H_0} \Big|_{H_0=H_0^*} = 0 \quad \text{or} \quad H_0^* = 1 - \sqrt{\frac{R_s}{R_L} + t_2 f} \quad (28)$$

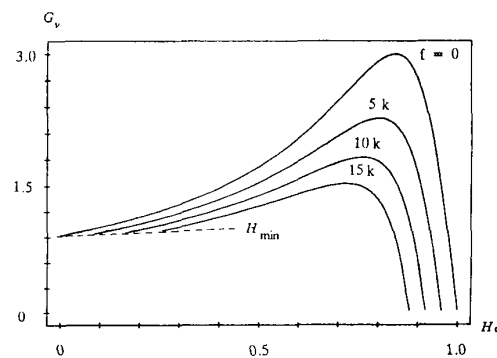


Fig. 6 DC gain degeneration of boost converter.

Then the maximum dc gain becomes

$$G_v(H_0^*) = \frac{1}{2\sqrt{\frac{R_s}{R_L} + (t_1 - t_2)f}} \quad (29)$$

It is obvious from (28) and (29) that the dc gain is deteriorated both by the conduction loss due to the inductor resistance R_s and by the switching loss due to the difference between voltage and current switching functions, $s_1(t) - s_2(t)$. However their effects are different. Hence it is not moderate to replace the switching effect with an equivalent resistance as done in [8] though this substitution gives somewhat similar result.

E. Efficiency Degeneration Effect

Efficiency η of the boost converter can be evaluated by comparing the input and output powers assuming low ripple.

$$\eta = \frac{P_o}{P_i} = \frac{Y_0^2/R_L}{U_0 X_1} \quad (30)$$

Evaluating X_0 from (19), Y_0 and X_1 are found to be

$$Y_0 = \frac{1 - H_0 + t_2 f}{\frac{R_s}{R_L} + (1 - H_0 + t_1 f)(1 - H_0 + t_2 f)} U_0 \quad (31a)$$

$$X_1 = \frac{1}{R_s + R_L(1 - H_0 + t_1 f)(1 - H_0 + t_2 f)} U_0 \quad (31b)$$

Then,

$$\eta = \frac{(1 - H_0 + t_2 f)^2}{R_s/R_L + (1 - H_0 + t_1 f)(1 - H_0 + t_2 f)} \quad (32)$$

To concentrate our attention to the switching effect only the inductor resistance R_s is set to zero. Then

$$\eta|_{R_s=0} = \frac{1 - H_0 + t_2 f}{1 - H_0 + t_1 f} \quad (33)$$

Efficiency degeneration by switching effect is depicted in Fig. 7. Remark on the fact that the efficiency is maximized when the dc gain is close to unity, which is the common properties of the dc converters. This result is similar to the result obtained in [7].

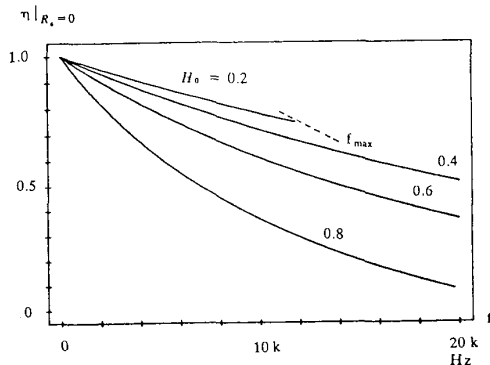


Fig. 7 Efficiency degeneration of boost converter.

III. BUCK CONVERTER MODELING

The buck converter as shown in Fig. 8 is modeled. The approach is very analogous to the boost converter case. Therefore detailed explanation is avoided here.

A. Exact State - Space Model

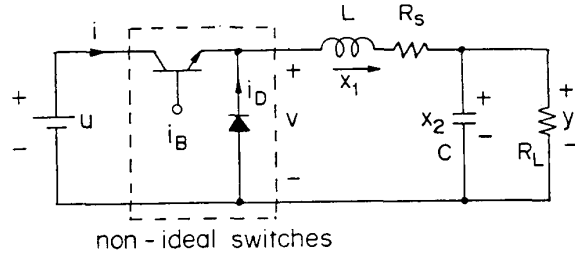


Fig. 8 Buck converter.

The state equation and the output equation are

$$\begin{bmatrix} \dot{x}_1 \\ \dot{x}_2 \end{bmatrix} = \begin{bmatrix} -\frac{R_s}{L} & \frac{1}{L} \\ \frac{1}{C} & -\frac{1}{CR_L} \end{bmatrix} \begin{bmatrix} x_1 \\ x_2 \end{bmatrix} + \begin{bmatrix} \frac{s_3(t)}{L} \\ 0 \end{bmatrix} u \quad y = [0 \ 1] \begin{bmatrix} x_1 \\ x_2 \end{bmatrix} \quad (34)$$

or

$$\dot{x} = Ax + B(t)u, \quad y = Cx \quad (35)$$

The $s_3(t)$ is found to be

$$s_3(t) = 1 - s_1(t) \quad (36)$$

Note that the $B(t)$ of the buck converter is time-varying instead of the $A(t)$ of the boost converter case.

B. State Space Averaging and Perturbation

The averaged matrices are

$$\bar{A} = A = \begin{bmatrix} -\frac{R_s}{L} & \frac{1}{L} \\ \frac{1}{C} & -\frac{1}{CR_L} \end{bmatrix}, \quad \bar{B} = \begin{bmatrix} \frac{s_3}{L} \\ 0 \end{bmatrix}, \quad \bar{C} = C = [0 \ 1] \quad (37)$$

and t_1, f are the same as (10). Then the perturbed matrices are

$$A_0 = A = \begin{bmatrix} -\frac{R_s}{L} & \frac{1}{L} \\ \frac{1}{C} & -\frac{1}{CR_L} \end{bmatrix}, \quad A_1 = A_2 = 0, \quad B_0 = \begin{bmatrix} \frac{H_0 - t_1 f}{L} \\ 0 \end{bmatrix}$$

$$B_1 = \begin{bmatrix} \frac{1}{L} \\ 0 \end{bmatrix}, \quad B_2 = \begin{bmatrix} \frac{dt_1}{dx_1} f \\ 0 \end{bmatrix}, \quad C_0 = C = [0 \ 1] \quad (38)$$

C. Switching Effects on Pole Frequency, DC Gain, and

Efficiency Degeneration

Characteristic equation is found to be

$$s^2 + \left(\frac{R_s^*}{L} + \frac{1}{CR_L} \right) s + \frac{1+R_s^*/R_L}{LC} = 0 \quad (39)$$

where

$$R_s^* = R_s + f \frac{dt_1}{dx_1} U_0 \quad (40)$$

There is pole frequency deviation due to the switching time modulation, which results in a variation of R_s to R_s^* . However there is no duty factor variation effect on pole frequency. Therefore it can be said that the buck converter is relatively strong against the switching effect.

DC gain is found to be

$$G_v = \frac{Y_0}{U_0} = -C_0 A_0^{-1} B_0 = \frac{R_L}{R_L + R_s} (H_0 - t_1 f) \quad (41)$$

The efficiency assuming low ripple is given by

$$\eta = \frac{P_o}{P_i} = \frac{Y_0 X_1}{U_0 I} = \frac{R_L}{R_s + R_L} \cdot \frac{H_0 - t_1 f}{H_0 - t_2 f} \quad (42)$$

The efficiency considering the switching loss only becomes

$$\eta \Big|_{R_s=0} = \frac{H_0 - t_1 f}{H_0 - t_2 f} \quad (43)$$

It can be seen that the efficiency becomes the maximum when the duty factor is unity. G_v, η are shown in Fig. 9 and Fig. 10 respectively.

IV. BUCK - BOOST CONVERTER

A. Exact State - Space Model

The state equation and output equation are found to be

$$\begin{bmatrix} \dot{x}_1 \\ \dot{x}_2 \end{bmatrix} = \begin{bmatrix} -\frac{R_s}{L} & -\frac{s_1(t)}{L} \\ \frac{s_2(t)}{C} & -\frac{1}{CR_L} \end{bmatrix} \begin{bmatrix} x_1 \\ x_2 \end{bmatrix} + \begin{bmatrix} \frac{s_3(t)}{L} \\ 0 \end{bmatrix} u, \quad y = [0 \ 1] \begin{bmatrix} x_1 \\ x_2 \end{bmatrix} \quad (44)$$

or

$$\dot{x} = A(t)x + B(t)u, \quad y = Cx \quad (45)$$

Note that $A(t)$ and $B(t)$ are exactly the same as those of the boost and the buck converters, respectively. Thus it is expected that the buck-boost converter is the general converter among the dc converters.

B. State - Space Averaging and Perturbation

The averaged and perturbed matrices are

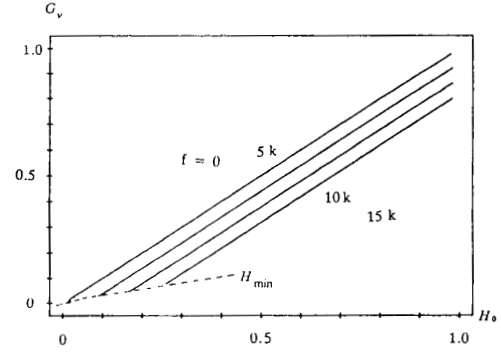


Fig. 9 DC gain deviation of buck converter.

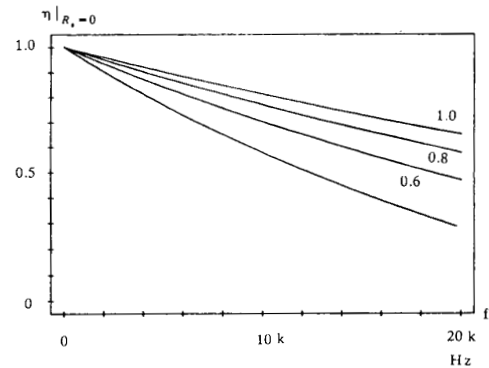


Fig. 10 Efficiency degeneration of buck converter.

$$\bar{A} = \begin{bmatrix} -\frac{R_s}{L} & -\frac{s_1}{L} \\ \frac{s_2}{C} & -\frac{1}{CR_L} \end{bmatrix}, \quad \bar{B} = \begin{bmatrix} \frac{s_3}{L} \\ 0 \end{bmatrix}, \quad \bar{C} = C = [0 \ 1] \quad (46)$$

and

$$A_0 = \begin{bmatrix} -\frac{R_s}{L} & -\frac{1-H_0+t_1 f}{L} \\ \frac{1-H_0+t_2 f}{C} & -\frac{1}{CR_L} \end{bmatrix}, \quad A_1 = \begin{bmatrix} 0 & \frac{1}{L} \\ -\frac{1}{C} & 0 \end{bmatrix},$$

$$A_2 = \begin{bmatrix} 0 & -\frac{f dt_1}{L dx_1} \\ \frac{f dt_2}{C dx_1} & 0 \end{bmatrix}, \quad B_0 = \begin{bmatrix} \frac{H_0 - t_1 f}{L} \\ 0 \end{bmatrix}, \quad B_1 = \begin{bmatrix} \frac{1}{L} \\ 0 \end{bmatrix}$$

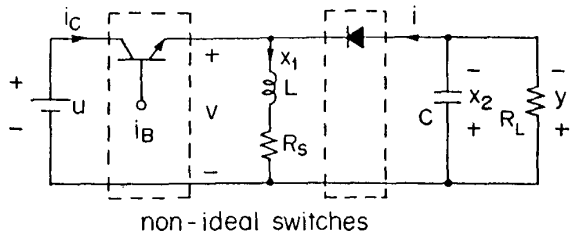


Fig. 11 Buck-boost converter.

$$B_2 = \begin{bmatrix} -\frac{dt_1}{dx_1} f \\ \frac{dt_1}{dx_1} L \\ 0 \end{bmatrix}, \quad C_0 = C = [0 \ 1] \quad (47)$$

C. Switching Effects on Pole Frequency, DC Gain, and Efficiency Degeneration

The characteristic equation is found to be the same as that of the boost converter with a slight modification of the value R_s^* .

$$R_s^* = R_s + f \frac{dt_1}{dx_1} (U_0 + X_2) \quad (48)$$

DC gain is given by

$$G_v = \frac{Y_0}{U_0} = \frac{(1-H_0+t_2f)(H_0-t_1f)}{\frac{R_s}{R_L} + (1-H_0+t_1f)(1-H_0+t_2f)} \quad (49)$$

The tendency is much similar to the boost converter case.

The efficiency assuming low ripple is given by

$$\eta = G_v \cdot \frac{I}{I_c} = \frac{(H_0-t_1f)(1-H_0+t_2f)^2}{\left[\frac{R_s}{R_L} + (1-H_0+t_1f)(1-H_0+t_2f) \right] (H_0-t_2f)} \quad (50)$$

The efficiency considering the switching loss only becomes

$$\eta \Big|_{R_s=0} = \frac{H_0-t_1f}{1-H_0+t_1f} \cdot \frac{1-H_0+t_2f}{H_0-t_2f} \quad (51)$$

Note that (51) is just the product of the efficiencies of the buck and boost converters. So the efficiency of the buck-boost converter is the lowest one. And the maximum efficiency is obtained at H_0^* given by

$$\frac{\partial \eta}{\partial H_0} \Big|_{H_0=H_0^*} = 0 \quad \text{or} \quad H_0^* = \frac{1+(t_1+t_2)f}{2} \quad (52)$$

Therefore the maximum efficiency is

$$\eta_{\max} = \eta \Big|_{H_0=H_0^*} = \left[\frac{1-(t_1-t_2)f}{1+(t_1-t_2)f} \right]^2 \quad (53)$$

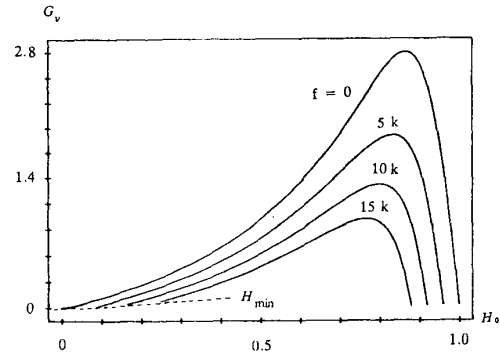


Fig. 12 DC gain degeneration of buck-boost converter.

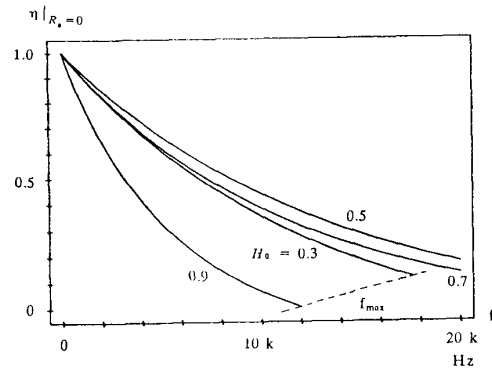


Fig. 13 Efficiency degeneration of buck-boost converter.

V. SUMMARY

Important results are tabulated using the normalized resistance r and the average switching functions s_1, s_2, s_3 and s_4 only. The results are very simple and regular in spite of the very complex switching waveforms and the exact description. In a whole, the properties of the buck or boost converters are the special cases of the general converter, buck-boost converter. The pole frequency, dc voltage gain, dc current gain and efficiency of the buck or boost converters are those of the buck-boost converter whose s_1, s_2 or s_3, s_4 are set to 1's, respectively.

Furthermore those of the buck-boost converter is just the products of those of buck converter and those of boost converter if the inductor resistance is neglected.

VI. CONCLUSION

The extension and generalization of the state-space average modeling to the non-ideal switching case and the unification and extension of the previous works have been performed. The switching effects on the system stability, dc gain and effi-

Table. Summaries of switching effects

type	Buck	Boost	Buck-boost
items	F_1	F_2	F_3
state eq.	A, B(t)	A(t), B	A(t), B(t)
ω_n^*	1	$\sqrt{\frac{r^* + s_1 s_2^*}{r^* + 1}}$	$\sqrt{\frac{r^* + s_1 s_2^*}{r^* + 1}}$
ζ^*	1	$\sqrt{\frac{r^* + 1}{r^* + s_1 s_2^*}}$	$\sqrt{\frac{r^* + 1}{r^* + s_1 s_2^*}}$
G_v	$\frac{s_3}{r+1}$	$\frac{s_2}{r+s_1 s_2}$	$\frac{s_2 s_3}{r+s_1 s_2}$
$G_v _{r=0}$	s_3	$\frac{1}{s_1}$	$\frac{s_3}{s_1}$
$G_i = -\frac{I_o}{I_i}$	$\frac{1}{s_4}$	s_2	$\frac{s_2}{s_4}$
$\eta = G_v, G_i$	$\frac{s_3}{(r+1)s_4}$	$\frac{s_2^2}{r+s_1 s_2}$	$\frac{s_2^2 s_3}{(r+s_1 s_2)s_4}$
$\eta _{r=0}$	$\frac{s_3}{s_4}$	$\frac{s_2}{s_1}$	$\frac{s_2 s_3}{s_1 s_4}$
$F_1 = F_3 _{s_1, s_2=1}$		$F_2 = F_3 _{s_3, s_4=1}$	
$F_3 _{r=0} = F_1 _{r=0} \cdot F_2 _{r=0}$			
$r = R_d/R_L, r^* = R_4^*/R_L, s_1 = 1 - H_0 + t_1 f,$ $s_2 = 1 - H_0 + t_2 f, s_2^* = 1 - H_0 + t_2^* f,$ $s_3 = H_0 - t_1 f, s_4 = H_0 - t_2 f$			

ciency for the buck, boost and buck-boost converters are explored.

The stabilities of all converters are affected by the switching time modulation effect which results in the variations of R_s and t_2 . And those of the boost and buck-boost converters are also affected by the average duty cycle variation effect due to finite switching times. In the sense of stability the buck converter is strong against switching effect, however the boost and buck-boost converters are weak in general and this becomes dominant when duty cycle approaches to unity.

The dc gains of the boost and buck-boost converters are deteriorated by the inductor resistance and the switching loss. And this effect becomes dominant also when duty cycle approaches to unity. So it is preferable to use the buck converter instead of other converters to avoid serious switching effects on dc gain. And it is needed especially to avoid unity duty cycle for the boost and buck-boost converters.

The efficiencies of all the converters are maximized when their dc gains are close to unity. It is recommended to avoid the buck-boost converter for higher efficiency.

So it can be concluded that the optimal duty factor of the buck converter is near unity, that of the boost converter is near zero and that of the buck-boost converter is near half, respectively.

It is believed that the analysis results are very helpful for the high frequency or high power applications and for the summary of the switching effects on the system stability, dc gain and efficiency.

REFERENCES

[1] R. D. Middlebrook and S. Cuk, "A general unified approach to modeling switching converter stages," in *IEEE Power Electronics Specialists Conf. Rec.*, pp. 18-34, 1976.

[2] P. Wood, "General theory of switching power converters," in *IEEE Power Electronics Specialists Conf. Rec.*, pp. 3-10, 1979.

[3] G. Verghese and U. Mukherji, "Extended averaging and control procedures," in *IEEE Power Electronics Specialists Conf. Rec.*, pp. 329-336, 1981.

[4] G. C. Verghese, M. E. Elbuluk and J. G. Kassakian, "A general approach to sampled data modeling for power electronic circuits," *IEEE Trans. Power Electronics*, vol. PE-1, No. 2, pp. 76-89, April 1986.

[5] Khai D. T. Ngo, "Low frequency characterization of PWM converter," *IEEE Trans. Power Electronics*, vol. PE-1, No. 4, pp. 223-230, October 1986.

[6] W. M. Polivka, P. R. K. Chetty and R. D. Middlebrook, "State-space average modeling of converters with parasitics and storage-time modulation," in *IEEE Power Electronics Specialists Conf. Rec.*, pp. 219-243, 1980.

[7] G. Eggers, "Fast switches in linear networks," *IEEE Trans. Power Electronics*, vol. PE-1, No. 3, pp. 129-140, July 1986.

[8] R. C. Wong, G. E. Rodriguez, H. A. Owen, Jr. and T. G. Wilson, "Application of small signal modeling and measurement techniques to the stability analysis of an integrated switching-mode power system," in *IEEE Power Electronics Specialists Conf. Rec.*, pp. 104-118, 1980.

[9] J. Sebastian, J. Uceda, "The double converter: A fully regulated two-output DC-DC converter," *IEEE Trans. Power Electronics*, vol. PE-2, No. 3, pp. 239-246, July 1987.